Turkish Journal of Earth Sciences

Manuscript 1910

# A two-stage deformation of the Anatolian Plate deduced from Paleomagnetic signals: The initial age of the Anatolian's escape

MUALLA CENGİZ

SAVAŞ KARABULUT

Turkish Journal of Earth Sciences

http://journals.tubitak.gov.tr/earth/

Research Article

Turkish J Earth Sci
(2024) 33: 243-259
© TÜBİTAK
doi:10.55730/1300-0985.1910

# A two-stage deformation of the Anatolian Plate deduced from Paleomagnetic signals: The initial age of the Anatolian's escape

Mualla CENGİZ[1,*], Savaş KARABULUT[2]

[1]Department of Geophysical Engineering, Faculty of Engineering, Istanbul University-Cerrahpaşa, İstanbul, Turkiye

[2]Department of Civil Engineering, Gebze Technical University, Kocaeli, Turkiye

**Received:** 07.06.2023 • **Accepted/Published Online:** 11.12.2023 • **Final Version:** 19.03.2024

**Abstract:** The Neotectonic period of deformation in Anatolia has been embraced by a location between the complex interaction of Afro-Arabian and Eurasia plates. During this ongoing deformation, the eastern part was under the continuing influence of subduction by the Neotethyan Ocean in the Eastern Mediterranean Region resulting in the indentation of the Arabian Plate into Anatolia. As the Red Sea opened deformation became increasingly focused on a fault system comprising the Dead Sea, North Anatolian, and East Anatolian fault systems. To help constrain the age and deformation history of this last phase we have conducted a paleomagnetic study from a total of 28 sites at Lower-Middle Miocene Mazgirt volcanic rocks and Pliocene Karakoçan basalts in the Anatolian Plate, and the Quaternary Cizre basalts of the Arabian Plate. The mean paleomagnetic direction in Early-Middle Miocene time identifies a clockwise rotation of 12.38° ± 5.1° in the Anatolian Plate. In contrast, counterclockwise rotation of 19.2° ± 6.1° and 14.8° ± 5.7° is obtained in the Middle Miocene-Pliocene and Quaternary periods in the Anatolian and Arabian Plate, respectively. According to our findings, we point to the importance of two distinct tectonic events. The first phase defines a period between Lower Miocene to Pliocene which is defined by a clockwise rotation of 31.5°. It is concluded that during this time interval, the collision between Arabia and Eurasia and the motion of Arabia in the northeast direction gave rise to the clockwise rotation of Anatolia. The North Anatolian Fault (NAF) is thought to be inactive, while the East Anatolian Fault (EAF) was not generated in this time interval. In the second phase, the northwest-directed movement of the Arabian Plate led to counterclockwise rotations both in the Anatolian and Arabian Plate. We suggest that the North Anatolian Fault provided a contribution to this movement in the Pliocene, while the East Anatolian Fault accompanied this tectonic westward escape of the Anatolian Plate after the Quaternary.

**Key words:** Anatolian-Arabian plate, paleomagnetism, NAF-EAF, westward escape, lower Miocene-Pliocene

## 1. Introduction

The Anatolian plate which occupies the 1500 km long segment of the Alpine–Himalayan Mountain chain in Türkiye, is composed of different tectono-stratigraphic domains showing several morphotectonic phases during the Neotectonic period in which the northward convergence between Arabia and Eurasia followed by westward extrusion of the Anatolian region by displacement along the North and East Anatolian Faults (Figure 1a; Şengör and Yılmaz, 1981; Okay, 1984; Bozkurt, 2001; Şengör et al., 2005; Yılmaz, 2019). The contemporary deformation of Anatolia is identified from GPS data which show a westwards motion of 20–25 mm/yr (McClucky et al., 2000; Reilinger et al., 1997a; Reilinger et al., 2006; Ergintav et al., 2023). Western Anatolia shows a very fast approximately N–S directed extension at a rate of 30–40 mm/yr (McKenzie, 1978; Jolivet et al., 2009), in contrast, Eastern Anatolia (Figure 1b) is a plateau that shows compression with high uplift rates of an average surface elevation of ~2 km above the sea level today (Şengör and Kidd, 1979; Pearce et al., 1990; Keskin, 2003). The collision of Arabia with Eurasia along the Bitlis-Zagros Suture Zone (BZSS) started shortly after the consumption of the southern branch of the Neotethys Ocean (Hall, 1976; Berberian and King, 1981; Dewey et al., 1986; Yılmaz, 1993; Jolivet and Faccenna, 2000; Robertson et al., 2007; Lebedev et al., 2016). Thus, crustal shortening in Eastern Anatolia and further north in Lesser/Great Caucasus has continued at a velocity of 18 mm/yr and 10 ± 2 mm/year, respectively due to the NW-directed movement of the Arabian Plate (McClusky et al., 2000).

The lithospheric deformation inside the collision zone in Eastern Anatolia has been investigated by numerous studies (Zor et al., 2003; Türkoğlu et al., 2008; Skobeltsyn et al., 2014; Mahatsente et al., 2018; Medved et al., 2021; Şengül Uluocak et al., 2021), however, the most surprising

* Correspondence: mualla@istanbul.edu.tr

evidence was the result of Sandvol et al., (2003), who argued that the lithospheric mantle is very thin under the collision zone in a wide area and that the ~45 km thick crust is present directly almost above the asthenosphere. The most common model involves slab steepening and the break-off of a northward subducting slab, which allows retention of the molten asthenospheric material beneath Eastern Anatolia (Keskin, 2003; Şengör et al., 2003; Facenna et al., 2006). During the late Miocene–Quaternary period, the whole of Eastern Anatolia was subject to intensive magmatic activity related to collision (Figure 1b) (Innocenti et al., 1976; Pearce et al., 1990; Yılmaz, 1990b; Yılmaz et al., 1998; Keskin et al., 1998; Özdemir and Güleç, 2014; Karaoğlu et al., 2020). The ongoing northward motion of Arabia into the Anatolian collage led to the generation of the North Anatolian Fault (NAF), the East Anatolian Fault (EAF), and the Dead Sea Fault (DSF).

Estimates for the age of initiation of the NAF range from late (middle) Miocene (Şengör and Kidd, 1979), 13–11 Myr. (Şengör et al., 2005) or 5 Myr (Barka and Kadinsky Cade, 1988; Bozkurt and Koçyiğit, 1996). The age of the East Anatolian Fault is reported to be Late Miocene-Early Pliocene (Şengör et al., 1985; Hempton, 1987) or less than 4 Ma (e.g. Şaroğlu and Yılmaz, 1990b; Westaway and Arger, 1996; Emre and Duman, 2007; Hubert Ferrari et al., 2009). The NAF and EAF intersect at the Karlıova region define a triple junction and accommodate in the east the continental shortening which is transformed into the westward escape in Western Anatolia (Figures 1a,1b). Another triple junction was defined between Anatolia-Arabia-Africa in the Maraş region where the northernmost branch of the DSF intersects the EAF (e.g., Karig and Kozlu, 1990). The development of these faults has created an escape tectonism of Anatolia along the Aegean arc in which the north–south compression was compensated.


**Figure 1.** a) Tectonic map of the Anatolia and surrounding (after National Oceanic and Atmospheric Administration (NOAA)), showing the GPS vectors together with their error ellipses at 95%confidence level after Reilinger et al., (1997b) (the study area is shown as a rectangle). b) Neotectonic map of Eastern Anatolia (gray areas indicate the distribution of Neogene volcanic rocks) (modified after MTA, geological map of 1/500,000 scale).

Significant paleomagnetic data have been provided in the Anatolian and Arabian Plates between the BZSZ, showing the presence of the westwards excursion of the Anatolia during the Miocene (Kissel et al., 2003; Tatar et al, 2004; Gürsoy et al., 2009). The paleomagnetic study of Koçbulut et al. (2013), however, showed that consistent counterclockwise rotation in the range of 5°–10° occurred off the Arabian Plate and was concentrated within the last 2–3 Myr with insignificant rotation from Miocene to the present. The collision between Arabia and Anatolia along the BZSZ and the behavior of the continental blocks during this time is still debated (Jolivet and Facenna, 2000; Cavazza et al., 2015; Darin and Umhoefer, 2022). To improve our understanding of the geodynamic evolution of the Arabian and Anatolian plates during Lower-Middle Miocene present we have undertaken new paleomagnetic studies in the region lying immediately to the west of the NAF-EAF junction (Figure 2a).

**2. Regional geology and paleomagnetic sampling**

The oldest rocks cropping out in the Eastern Taurides comprise an allochthonous nappe succession of the metamorphosed Permian-Late Cretaceous Keban Formation (Perinçek, 1979; Kaya, 2016). Upper Cretaceous ophiolitic rocks resulted from the closure of the northern and southern branches of the Neotethys ocean surrounding the study area in the north (Şengör and Yılmaz, 1981; Okay, 1984; Parlak et al., 2013) and south (Parlak et al., 2009; Karaoğlan et al., 2016) (Figure 2a). The uplift and deposition of sedimentary units started with conglomerates in the Lower Paleocene (Perinçek, 1979). The erosional surface consists of an Eocene-Oligocene flysch succession up to early Miocene continental sedimentary rocks (Perinçek, 1979).

Geochronologic data from Eastern Anatolia have shown that volcanism comprising andesite and rhyolite volcanic suites commenced in the south of the region at 15.0–13.5 Ma (Lebedev et al., 2010). Volcanism with the eruption of acid pyroclastic fall units and ignimbrites intensified in the northeast from 8 to 6 Ma. Volcanism continued during the Quaternary in the southern part of Eastern Anatolia with the eruption of basalts and trachybasalts from several eruption centers. From southwest to northwest, these are the Nemrut volcano with a 7 km wide caldera, the Süphan strato-volcano, the Etrüst strato and Girekol miniature shield volcano, the Tendürek shield volcano and the Greater and Lesser Ararat peaks located by the Armenian-Iranian border (Figure 1b). The last eruption in the region occurred from an N-S extending fissure cutting a small scoria cone in the north of the Nemrut caldera in 1441 AD (Yılmaz et al., 1998). During this historical eruption, alkaline basaltic lavas erupted following blocky rhyolitic lavas.

During this study, Lower Miocene-Middle Miocene volcanic rocks from Mazgirt (GD6-10; SE 12-14, 16) and Pliocene Karakoçan basalts (GD11-15; SE 22-26) were sampled around Tunceli, while Quaternary basalts were sampled in Cizre (GD1-5; TL 27, 28, 33-34) (Figures 2a, 2b).

The earliest volcanic activity in Tunceli is defined by andesites and volcanoclastic rocks, tuffs, and agglomerates of the Mazgirt lavas (Herece and Acar, 2016; Agostini et al., 2019). The Mazgirt volcanic rocks represent two main phases including lava domes fractured with columnar jointing/lava flows and associated pyroclastic products. Above the Mazgirt volcanic succession, another distinct volcanic phase is defined by the Tunceli volcanic rocks which are composed largely of basaltic subhorizontal lava flows with a total thickness of less than 100 m (Agostini et al., 2019). The last phase is represented by the Karakoçan volcanic rocks which contain alkali basalts, hawaiites, and mugearites showing weakly porphyritic to subaphyric lavas (Agostini et al., 2019). $^{40}$Ar-$^{39}$Ar ages indicate an eruption age of ~16.3 and 15.1 Ma for the Mazgirt volcanic activity. The basaltic lava flows yield a $^{40}$Ar-$^{39}$Ar age of ~11.4–11.0 Ma in Tunceli and ~4.1 Ma for the Karakoçan volcanic flow (Agostini et al., 2019).

The youngest lavas in the Southeastern Anatolia which belong to the Arabian Plate are the Quaternary basalts in Cizre (Figures 2a, 2b). The basalts uncomfortably overlie the limestones of the Oligocene sedimentary succession of the Midyat Group assigned to the beginning of the Quaternary (Figure 2b). A possible source of the basalts is Mount Alem in the vicinity of Cizre district (MTA, 2007). Pliocene deposits belong to the youngest lavas of Southeastern Anatolia (Tolun, 1960) and the thickness of this basalt is no more than 20 m. The thickness of this basalt structure reaches 20 m in places.

**3. Methodology**

Orientated core samples were taken with a motorized portable drill and cut into cylindrical specimens of 2.5 cm diameter and 2.2 cm length. Sample orientation was determined using both magnetic and sun compasses. The differences of about 2°–10° of the readings between the magnetic and sun compass were recalculated by the strike orientation. The majority of a total of 266 specimens from 28 sites was subjected to stepwise alternating field (AF) demagnetization , while thermal demagnetization showed anomalous behavior. The directions and intensities of the natural remanent magnetization (NRM) were measured using a JR-6 spinner magnetometer (AGICO) in the Yılmaz Ispir Paleomagnetism Laboratory of İstanbul University-Cerrahpaşa, Türkiye. A decaying alternating field between 2.5 and 150 mT was applied using a 2G600 AF demagnetizer, while temperatures between 50 °C and 700 °C were applied using a Magnetic Measurements MTD-80 oven. An orthogonal vector projection was used

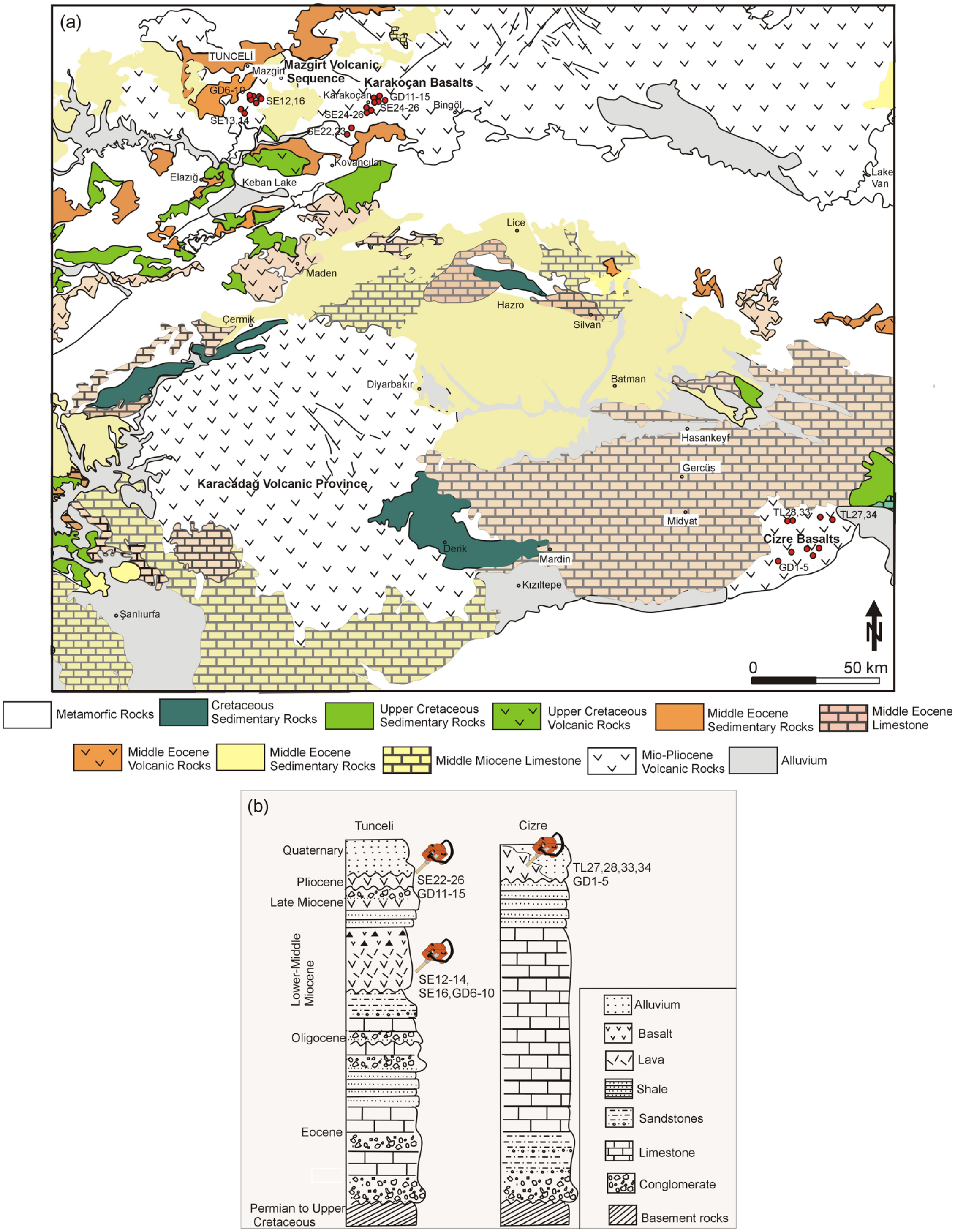


**Figure 2. a)** Geological map of the study area (modified after MTA, 2002; geological map of 1/500,000 scale). Paleomagnetic samples are collected from the Mazgirt, Karakoçan, and Cizre volcanic areas. b) Stratigraphic column section of the study area in Tunceli and Cizre.

to identify the magnetization components (Zijderveld, 1967) and the magnetization directions were calculated using principal component analysis (Kirschvink, 1980). Mean directions and statistical analysis were applied using Fisher's (1953) analysis. The paleosecular variation (PSV) test was applied by using the criteria of Deenen et al. (2011). Thermomagnetic measurements in low field susceptibility were applied to each pilot sample using an MS2 Bartington susceptibility meter. Isothermal remanent magnetization (IRM) was conducted by applying fields up to 1 T. The Lowrie test (Lowrie, 1990) was performed by applying fields of 1 T along the sample Z-axis (hard component), 0.4 T (medium component) along the Y-axis, and 0.12 T (soft component) along the X-axis. Afterward, these samples were thermally demagnetized to determine their unblocking temperatures.

## 4. Laboratory analysis

### 4.1. Rock magnetism

Thermomagnetic results of basalt samples are characterised by nearly reversible susceptibility curves confirming no mineralogical alteration. Curie temperatures are between 500 and 580 °C, indicating that Ti-poor titanomagnetite is most probably the dominant ferromagnet (Figures 3a, 3b, 3c). Representative IRM acquisition (Figures 3a, 3b, 3c) and thermal decay (Figures 3d, 3e, 3f) experiments indicate a rapid rise of magnetization to about 300 mT in general (Figures 3d, 3f), or a slower increase to 500 mT (Figure 3e) suggesting the existence of low-coercivity minerals. Thermal demagnetization of three-component IRM shows that the low-coercivity component unblocked by 500 °C and 550 °C, showing the presence of Ti-poor magnetite (Figures 3g, 3h, 3i). In site SE34 (Figure 3i), however, a decrease from 75 °C to 150 °C could be associated with the existence of goethite, as seen by a similar decrease on the Curie curve (Figure 3c).

### 4.2. Demagnetization

Initial magnetic intensities of the basalt and andesites are in the range of 200–9000 mA/m. Lower remnant intensities are compatible with mineralogy, being lower in higher Na+K compositions. Characteristic remanence (ChRM)

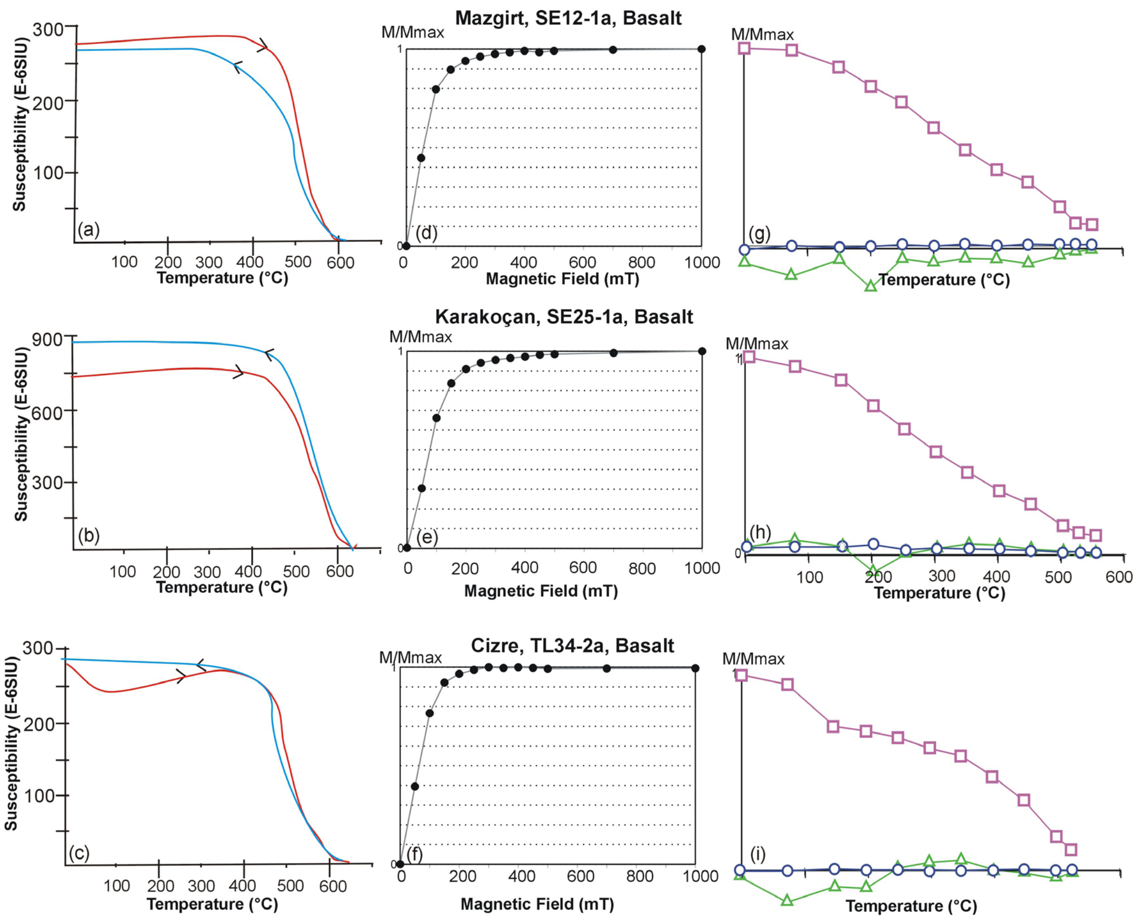


**Figure 3.** Typical thermomagnetic curves for representative samples (a, b, c). Normalized IRM acquisition curves (d, e, f). Thermal demagnetization of three-axis IRM imposed with the direct field of 1 T along the z-axis (circles), 0.4 T along the y-axis (triangle), and 0.12 T along the x-axis (square) (g, h, i).

directions are resolved with Medium Destructive Field (MDF) values of 10–30 mT (Figure 4) and their directions identified from vector endpoint diagram segments converging towards the projection origins (Figures 4a–4g) following the removal of low coercivity components.

The relatively lower intensity values are compatible with the mineral compositions containing higher Na+K composition, i.e. the Karakoçan basalts (Agostini et al., 2019). Characteristic remanence (ChRM) directions are defined with a Medium Destructive Field (MDF) value of 10–30 mT (Figure 4). The ChRM direction is identified in the vector endpoint diagrams (Zijderveld, 1968) aligned toward the origin (Figures 4a–4g) following the removal of a low coercivity remanence (0–10 mT) (Figures 4h–4l, 4n, 4o) during demagnetization. Thermal demagnetization yielded less satisfactory results probably due to narrow unblocking temperatures and therefore less satisfactory component definitions on vector diagrams (Figure 4o). Results from AF demagnetization have therefore been mostly used in this analysis.

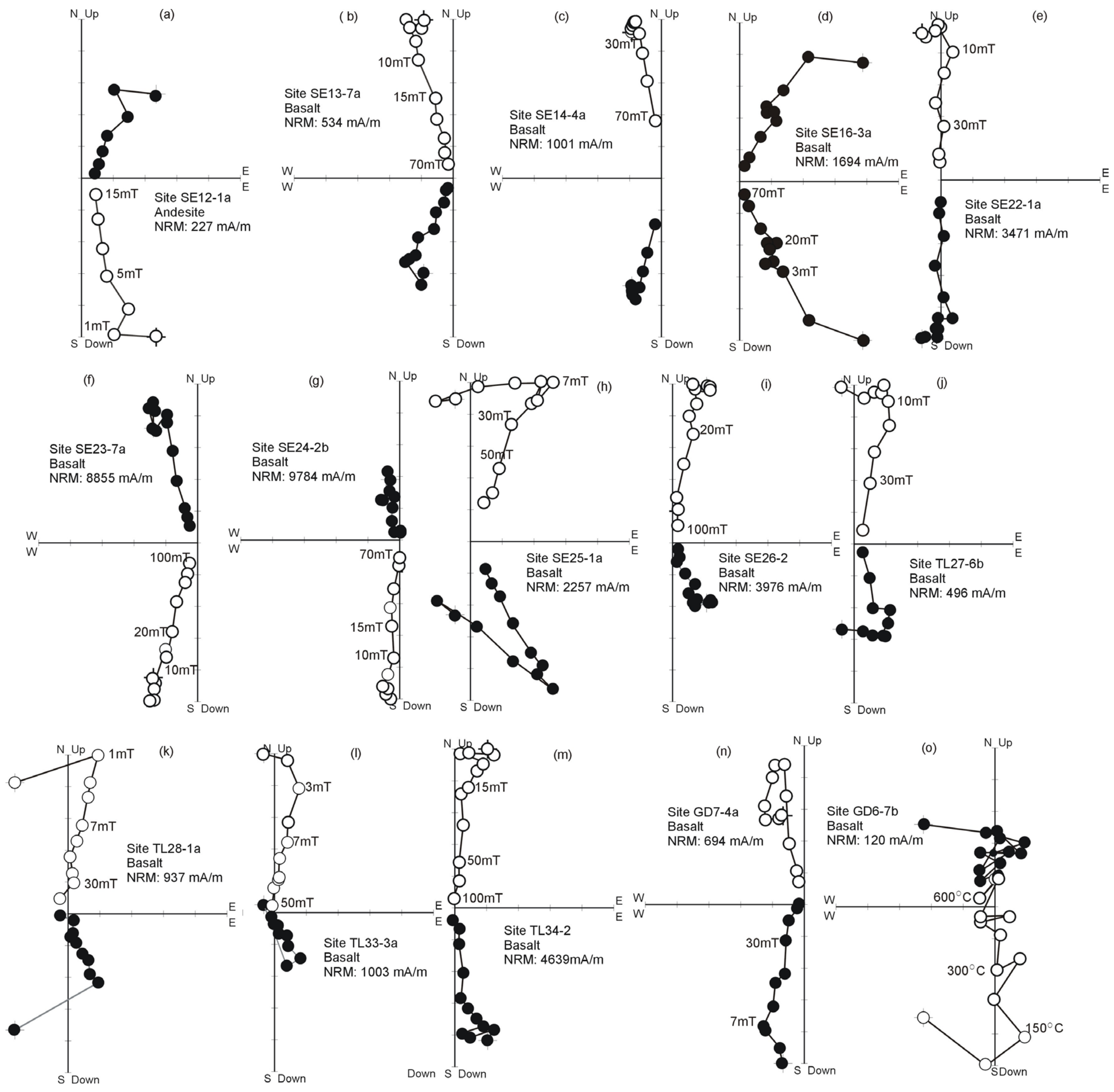


**Figure 4.** NRM intensities and orthogonal vectors of representative samples during stepwise alternating field (a–n) and thermal (o) demagnetization (in miliTesla (mT) and degrees Celsius). The solid symbols correspond to projections onto the horizontal plane, while the open symbols are projections onto the vertical plane.

## 5. Discussion

### 5.1. Paleomagnetic directions

Stable ChRM site mean directions were obtained with confidence circles ($\alpha_{95}$) of less than 8° (Table). The inclinations for several sites indicate mixed polarities in several sites (Figure 5). Coherent inclination values are comparable with the present predicted field direction in this region (Table).

From a total of 28 sites, group mean directions were calculated for three distinct ages and areas. There is a clear difference in paleomagnetic directions according to age (Table). In the Anatolian Plate, Lower Miocene-Late Miocene lavas show an average group mean direction of D = 18.7° and I = 49.9° (k = 113.1, $\alpha_{95}$ = 4.9°, N:9 sites) and Pliocene lavas in the same area show a group mean direction of D = 342.3° and I = 49.6° (k = 58.0, $\alpha_{95}$ = 6.4°, N:10 sites). In the Arabian Plate, a group mean direction of D = 346.6° and I = 57.2° (k =121.9, $\alpha_{95}$ = 4.7°, N:9 sites) is calculated for Quaternary lavas. When these group mean directions are compared with their respective reference geomagnetic dipole fields of Eurasia for 0–10 and 20 Ma (Torsvik et al., 2012), rotations of 12.3° ± 5.1°, −19.2° ± 6.1°, and −14.8° ± 5.7° were detected, respectively (Table).

The mean inclinations (paleolatitude) from this study, however, indicate values in the order of 49.9° (30.7°N), 49.6° (30.4°N), and 57.2° (37.8°N) from Lower Miocene, Pliocene, and Quaternary rocks, respectively (Table). Although Abou Deeb and Tarling (2005) reported low inclination values from Miocene lavas in Syria and suggested that they were influenced by a strong and nondipole magnetic field of this age, we find no significant inclination flattening compared with the expected inclinations from the 0–10 and 20 Ma Eurasian Apparent Polar Wander Path (APWP) (Table).

### 5.2. Paleosecular variation

The temporal and spatial behavior of the palaeosecular variation (PSV) of the geomagnetic field can be estimated by the angular standard deviation of VGPs (Virtual geomagnetic pole) for a given locality of individual lava flows. The geomagnetic dispersion was calculated by the formula $S^2_B = S^2_T - S^2_w$, and $\sum S_T = \left[\left(\frac{1}{N}-1\right)\sum_{i=1}^{N}\delta_i^2\right]^{\frac{1}{2}}$ (Cox, 1969). The dispersion ($S_B$) is derived by subtracting the circular standard deviation of the VGP ($S_W$) from the total dispersion ($S_T$) (Cox, 1969) and the PMAG software (Tauxe, 2005). N defines the number in the calculation, while $\delta_i$ is the angular distance between the i$^{th}$ VGP and the reference axial dipole, and $S_T$ is the within–site dispersion (McElhinny and McFadden, 1997). The PSV is averaged out if the A95 angle lies between the lower (A95min) and upper (A95max) limits. In some sites where $A_{95}$ values were lower than $A_{95}$min, the specimen numbers were reduced to pass the Deenen et al., (2011) criteria, the lava flows from the three separated areas were emplaced over time intervals sufficiently long to embrace both normal and reverse geomagnetic field polarities and A95 values fall within the reliability envelope of Deenen et al., (2011) (Table).

### 5.3. Kinematic model

The collision of Arabia with Anatolia along the BZSS is inferred to have taken place by early to the middle Miocene (Şengör and Yılmaz, 1981; Dewey et al., 1986; Robertson et al., 2007; Okay et al., 2010; Cavazza et al., 2015, 2018; Lebedev et al., 2016). This age is supported by thermochronometric evidence for evolution along the Bitlis-Pütürge zone with the Oligocene rocks studied by Cavazza et al. (2018) indicating that the continental collision started in the mid-Miocene. However, several studies have inferred earlier ages of collision ranging from the Late Cretaceous (Hall, 1976; Berberian and King, 1981), middle Eocene, and late Oligocene time (Yılmaz, 1993; Jolivet and Faccenna, 2000; Vincent et al., 2007; Allen and Armstrong, 2008; Rolland et al., 2012; McQuarrie and van Hinsbergen, 2013) or a later Pliocene collision (Philip et al., 1989). McClusky et al. (2003) concluded that independent motion of the Arabian plate began in the late Oligocene.

Darin and Umhoefer (2022) suggested an initial "soft collision", of the thinned continental crust of the Arabian passive margin with Eurasia at ca. 42 Ma along the Eastern Bitlis Suture zone and continuing into a "hard collision" by ca. 25–12 Ma.

The Lower Miocene-Middle Miocene paleomagnetic result obtained from this study in the Anatolian Plate indicates a clockwise rotation of 12.3° ± 5.1° in the Lower-Middle Miocene. A significant amount of 31.5° clockwise relative rotation with respect to Africa is obtained between Lower-Middle Miocene and Pliocene contrasting with an inferred Pliocene rotation of −19.2° ± 6.1° in the same area.

Previous Neogene paleomagnetic results from the east of the Karlıova triple junction showed a significant amount of clockwise rotations, besides counterclockwise rotations in Miocene volcanic rocks (Hisarli et al., 2016). The origin of the contrasting sense of rotations in East Anatolia was interpreted by wedge-shaped crustal blocks separated by strike-slip faults during the Miocene to Quaternary (Hisarli et al., 2016). Kayın and İşseven (2023), however, paid attention to smaller blocks which moved in different directions, both clockwise and counterclockwise in this area.

Further northeast in the Talysh Mountains of NW Iran, van der Boon et al., (2017) reported a ~15° clockwise since the Eocene which is in the same direction as the Lower-Middle Miocene results of this study. In other words, the northern part of the BZSS has exhibited a

| Site | Latitude (°N) | Longitude (°E) | N/n | $D_g$ | $I_g$ | $\alpha_{95}$ | k | R±ΔR | F±ΔF | A95 | $A95_{min}$ | $A95_{max}$ |
|---|---|---|---|---|---|---|---|---|---|---|---|---|
| **Lower Miocene- Middle Miocene MAZGİRT LAVA** | | | | | | | | | | | | |
| GD6 | 38.984931 | 39.582657 | 11/10 | 14.1 | 52.1 | 5.7 | 73.1 | | | 5.7 | 4.6 | 18.1 |
| GD7+ | 39.001124 | 39.632075 | 12/7 | 195.8 | –62.5 | 4.1 | 222.6 | | | 5.68 | 5.51 | 24.1 |
| GD8+ | 39.009259 | 39.647110 | 8/6 | 27.2 | 39.2 | 7.1 | 89.9 | | | 5.87 | 5.86 | 26.5 |
| GD9 | 39.005850 | 39.634227 | 11/11 | 19.0 | 51.8 | 4.7 | 96.7 | | | 4.9 | 4.6 | 18.1 |
| GD10+ | 38.986064 | 39.630742 | 13/9 | 24.8 | 54.9 | 4.6 | 127.7 | | | 5.18 | 4.98 | 20.54 |
| SE12 | 38.976058 | 39.527570 | 9/8 | 9.8 | 44.0 | 5.9 | 90.5 | | | 5.5 | 5.2 | 22.1 |
| SE13 | 38.973640 | 39.528920 | 9/9 | 198.5 | –49.2 | 5.5 | 87.7 | | | 5.8 | 5.0 | 20.5 |
| SE14 | 38.970780 | 39.543000 | 9/9 | 201.7 | –48.6 | 6.3 | 68.2 | | | 7.0 | 5.2 | 22.1 |
| SE16 | 38.976431 | 39.626987 | 9/8 | 16.1 | 45.7 | 6.8 | 66.6 | | | 7.4 | 5.2 | 22.1 |
| | | **Mean N:9** | | **18.7** | **49.9** | **4.9** | **113.1** | **12.3 ± 5.1** | **5.9 ± 4.3** | | | |
| **Pliocene KARAKOÇAN LAVA** | | | | | | | | | | | | |
| GD11 | 38.964789 | 40.206897 | 9/9 | 342.4 | 44.2 | 6.8 | 58.4 | | | 6.3 | 5.0 | 20.5 |
| GD12+ | 38.915217 | 40.184928 | 9/7 | 341.5 | 40.3 | 6.6 | 83.5 | | | 5.6 | 5.5 | 26.1 |
| GD13+ | 38.914622 | 40.194011 | 8/6 | 345.3 | 40.9 | 7.7 | 76.6 | | | 6.6 | 5.9 | 26.5 |
| GD14 | 38.993849 | 40.072529 | 8/7 | 342.8 | 60.0 | 5.9 | 106.1 | | | 7.0 | 5.5 | 24.1 |
| GD15 | 38.997329 | 40.168103 | 8/8 | 157.6 | –47.8 | 5.5 | 103.5 | | | 5.4 | 5.2 | 22.1 |
| SE22 | 38.850090 | 39.992630 | 10/10 | 185.4 | –49.9 | 5.8 | 69.5 | | | 6.9 | 4.8 | 19.2 |
| SE23 | 38.888320 | 40.025370 | 9/9 | 338.0 | 35.7 | 6.4 | 66.4 | | | 6.1 | 5.0 | 20.5 |
| SE24 | 38.949210 | 40.118312 | 9/9 | 340.3 | 58.4 | 6.3 | 68.5 | | | 7.1 | 5.0 | 20.5 |
| SE25 | 38.951650 | 40.184600 | 9/8 | 153.2 | –55.8 | 4.2 | 176.3 | | | 5.2 | 5.2 | 22.1 |
| SE26 | 38.955600 | 40.134090 | 9/9 | 164.3 | –60.2 | 3.9 | 174.8 | | | 5.3 | 5.0 | 20.5 |
| | | **Mean N:10** | | **342.3** | **49.6** | **6.4** | **58.0** | **–19.2 ± 6.1** | **7.2 ± 5.3** | | | |

| | | | | | | | | | | | | |
|---|---|---|---|---|---|---|---|---|---|---|---|---|
| **Quaternary Cizre LAVA** | | | | | | | | | | | | |
| GD1 | 37.276724 | 41.998612 | 8/8 | 344.6 | 55.2 | 6.3 | 77.2 | | | 6.6 | 5.2 | 22.1 |
| GD2+ | 37.285068 | 42.262199 | 8/6 | 348.4 | 55.0 | 6.3 | 113.6 | | | 6.7 | 5.9 | 26.5 |
| GD3 | 37.224963 | 41.879876 | 7/7 | 345.1 | 40.4 | 7.8 | 61.5 | | | 6.2 | 5.5 | 24.1 |
| GD4+ | 37.267795 | 41.954555 | 11/8 | 347.7 | 61.8 | 4.9 | 131.8 | | | 5.7 | 5.2 | 22.1 |
| GD5 | 37.268095 | 42.132426 | 11/11 | 344.2 | 57.7 | 3.6 | 162.2 | | | 4.7 | 4.6 | 18.1 |
| TL27 | 37.341640 | 42.158880 | 11/8 | 166.8 | –59.0 | 3.3 | 285.8 | | | 6.3 | 5.5 | 24.1 |
| TL28 | 37.355790 | 41.939380 | 9/9 | 162.3 | –58.3 | 7.1 | 53.2 | | | 8.1 | 5.0 | 20.5 |
| TL33 | 37.355750 | 41.947140 | 10/10 | 167.2 | –65.6 | 3.6 | 184.8 | | | 4.8 | 4.8 | 19.2 |
| TL34 | 37.359660 | 42.026930 | 12/9 | 175.0 | –61.3 | 5.6 | 85.3 | | | 7.8 | 5.0 | 20.5 |
| | | **Mean N:9** | | **346.6** | **57.2** | **4.7** | **121.9** | **–14.8 ± 5.7** | **–1.5 ± 4.5** | | | |

**Table.** Paleomagnetic results from Lower-Middle Miocene, Pliocene and Quaternary lavas (site numbers, geographic location (latitude (°N), longitude (°E) are indicated in the Table, N shows the number of samples per locality, and n is the number of samples used for site mean calculation. The group mean directions are denoted in bold. Declination $D_g$ and inclination $I_g$ describe the mean directions in geographic coordinate, 95 is the 95% confidence circle, *k* is the precision parameter (Fisher, 1953). R and F are the angles of vertical axis rotation (positive indicates clockwise rotation) and flattening of inclination (±, northward/southward) with respect to the direction computed from the stable Eurasian paleomagnetic pole with 95% confidence limits R and F, respectively (after Demarest, 1983). The difference between the observed poles ( $_{obs}$, $_{obs}$) and the reference pole ( $_{ref}$, $_{ref}$), computed using the pole-space method of Beck (1980), defines the amount of vertical axis rotation (R) and poleward transport (F). A95 shows the angle of confidence of the VGP of each site, A95min, A95max are the minimum and maximum values of A95, after Deenen et al., (2011). (+) denote specimens of decreasing size to pass the Deenen et al., (2011) criteria.

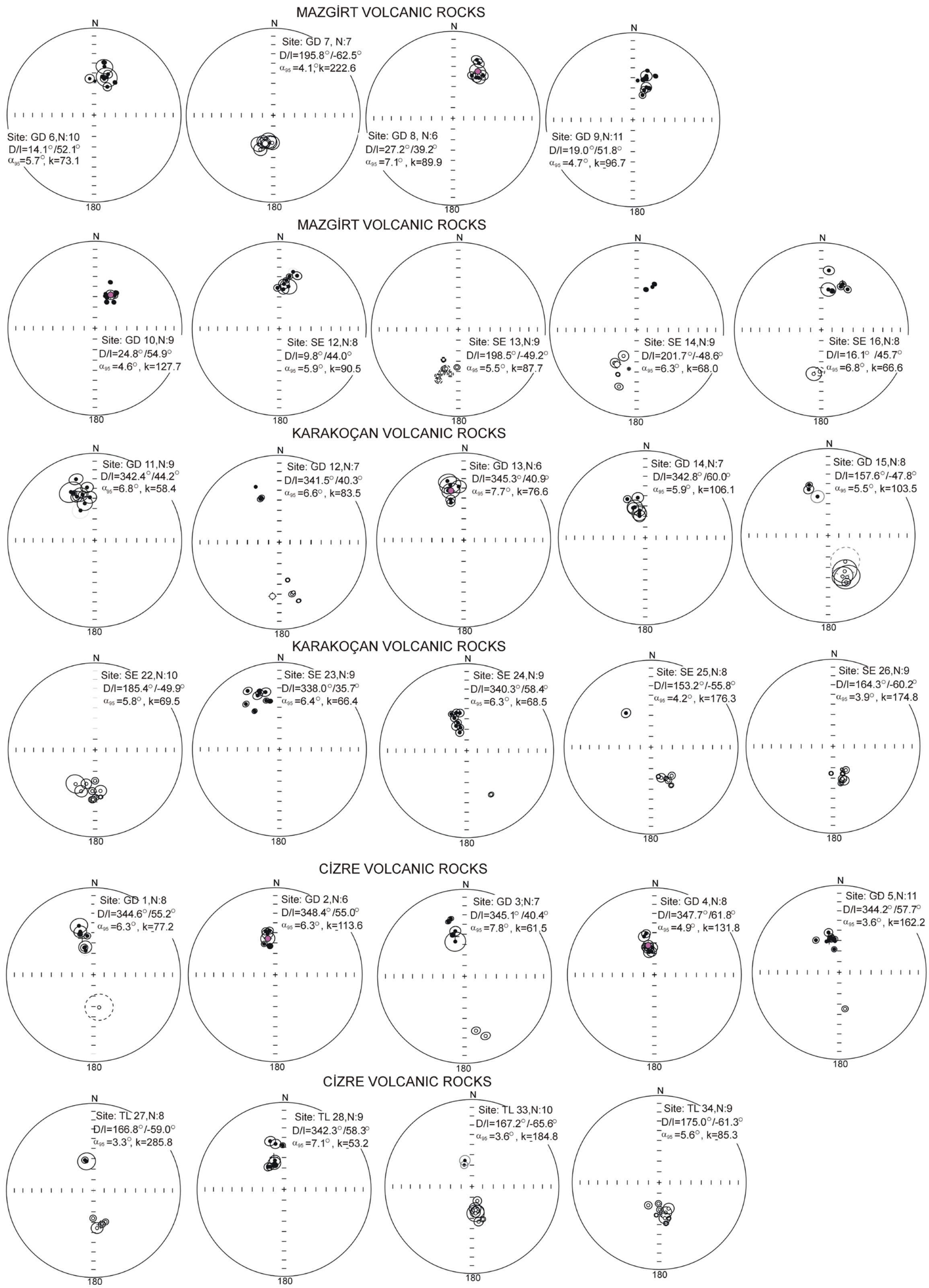


**Figure 5.** Paleomagnetic site mean directions (solid (open) symbols on the lower (upper) hemisphere of equal area stereographic projection).

regional clockwise character along the NE part of Iran and the Anatolian plate. In contrast, the southern part of this zone exhibited counterclockwise rotation during the Neogene Period which is as follows: In the Arabian Plate, Gürsoy et al., (2009) calculated a mean direction of 8.4/44.7 in Quaternary lavas, 350.0/50.3 in Late Miocene East Euphrates lavas and 356.8/51.5 in Gaziantep lavas. Koçbulut et al., (2013) calculated mean directions in the Arabian Plate which are as follows; D/I = 175°/–50.5° for the 11.1–6.7 Ma Siverek group, D/I = 173.4°/–46.0° for the 3.3 Ma central Karacadağ group and D/I = 167.7°/–47.6° for the ~ 1.9 Ma-present Ovabağ group.

We interpret the contrasting sense of rotations between the northern and the eastern part of the BZSS as a result of the opening of the Red Sea and the evolution of the Dead Sea Fault due to the movement between Africa and Arabia which affected most of the western margin of the Arabian Plate. Several paleomagnetic studies show both clockwise and counterclockwise rotation from Lebanon, Jordan, and Israel (Henry et al., 2010; Dembo et al., 2021), while in the south of the Arabian Plate, paleomagnetic results from Saudi Arabia and Syria are directed close to an N-S azimuth during the Lower Miocene and show no signature of significant rotation (Kellogg and Reynolds, 1983; Roperch and Bonhommet, 1986).

In the Anatolian Plate, Miocene data from the Anatolian Plate report a general counterclockwise rotation east of the Isparta angle (e.g., Gürsoy et al., 1997; Kissel et al., 2003; Gürsoy et al., 2011). In the study of Gürsoy et al., (2011) volcanic rocks dated ~15– 13.5 Ma in the area between the Central Anatolian and East Anatolian Fault Zones identify counterclockwise rotation of 29.3 ± 5.2° and 26.0 ± 11.8° from the Yamadağ and Kepezdağ complexes (Figure 1b) respectively relative to Eurasia. The new paleomagnetic results from the western border of the Eastern Anatolia plate show clockwise rotation in Lower-Middle Miocene and counterclockwise rotation in Pliocene and Quaternary time (Figure 6a). The results display a dominant clockwise rotation of ca. 33° between Lower- Middle Miocene and Pliocene. The contrasting senses of rotation identified from two different time intervals are interpreted in terms of two distinct tectonic phases affecting the area.

**1) Collision among Africa-Arabia-Anatolia:** Kinematic models of plate motion show a northeastward movement of Africa-Arabia (Figure 6b). This movement is reported as lasting until the Middle Miocene (Matthews et al., 2016; Darin and Umhöfer 2022) or Burdigalian with an average velocity of 2.4 cm/yr (Cavazza et al., 2018). The clockwise rotation in the Lower-Middle Miocene confirms this direction (Figure 6c). Darin and Umhöfer (2022) reported a diachronous collision depending on the irregular geometry of the Arabian margin as this region experienced a confluence of major tectonism including oceanic subduction, continental underthrusting, and crustal shortening. The collision was along the BZSS from ca. 35–20 Myr. The collision on the Zagros suture towards the southeast, however, is reported as occurring between 27 and 18 Ma (McQuarrie et al., 2003; McQuarrie and van Hinsbergen 2013; Su and Zhou 2020). The onset of the continental hard collision along BZSZ is dated ~19 Myr and the initiation of collision is related to the uplift in East Anatolian (Gülyüz et al., 2020).

The African plate was broken up in the Oligocene-early Miocene by the opening of the Red Sea (Hempton, 1987; Ibrahim et al., 2000). After this time, the Arabian Plate moved faster than the African Plate (Africa / Eurasia relative motion: 1.7 cm/yr, Arabia/Eurasia relative motion: 2.4 cm/yr; Cavazza et al., 2018). Jolivet and Faccenna (2000) showed that the extension in the Mediterranean due to the initiation of the Nubia/Arabia–Eurasia collision caused the slowing of Nubia absolute plate motion. Mantovani et al., (2006) reported that the shortening along the BZSS was not restricted to the late Miocene-Pliocene and an early–middle Miocene shortening should also be considered. Our results indicate that the North and East Anatolian Faults were either not formed or were not active, since the paleomagnetic rotations are in accordance with the motion of the Arabian-African Plate in a clockwise sense during the Early-Middle Miocene.

**2) Indentation of Arabia**: The main source of Anatolian escape is the northern indentation of Arabia along the BZSZ. Hüsing et al., (2009) date the youngest sediments in the Arabian Plate beneath a subduction-related thrust at ca. 11 Ma and suggest that the subduction of Arabia ended during this time. Facenna et al., (2006) note that collision had already been achieved before the onset of the NAF, while Ergintav et al., (2023) reported that the North and East Anatolian Faults controlled the recent deformation of Anatolia during the interval 5–10 Myr. Whitney et al., (2023) showed that the EAF in Southeast Anatolia was active over the past ~5 m.y. and obtained younger thermochronology data than in other fault zones in the region. We conclude that after the Pliocene, the NAF had gained its present characteristics, while later after the Quaternary the EAF accommodated the deformation attributed to the "tectonic escape". This was confirmed by the clockwise rotations of 31.5° in the Anatolian Plate during Lower-Middle Miocene to Pliocene (Figure 6c) and the counterclockwise rotations of 19.2° and 14.8° during Pliocene and Quaternary resolved from both the Arabian and Anatolian Plate, respectively (Figure 6d). The difference between the rotations of Anatolia and Arabia in Pliocene and Quaternary is 4°, respectively (Table). This is interpreted in terms of a) active Neotectonic faulting in Anatolia, while Arabia remained essentially stable; b) motion of the Anatolian Plate reported at a rate of 1° per 1 mm/yr (Gürsoy et al. 2009), c) underthrusting of the

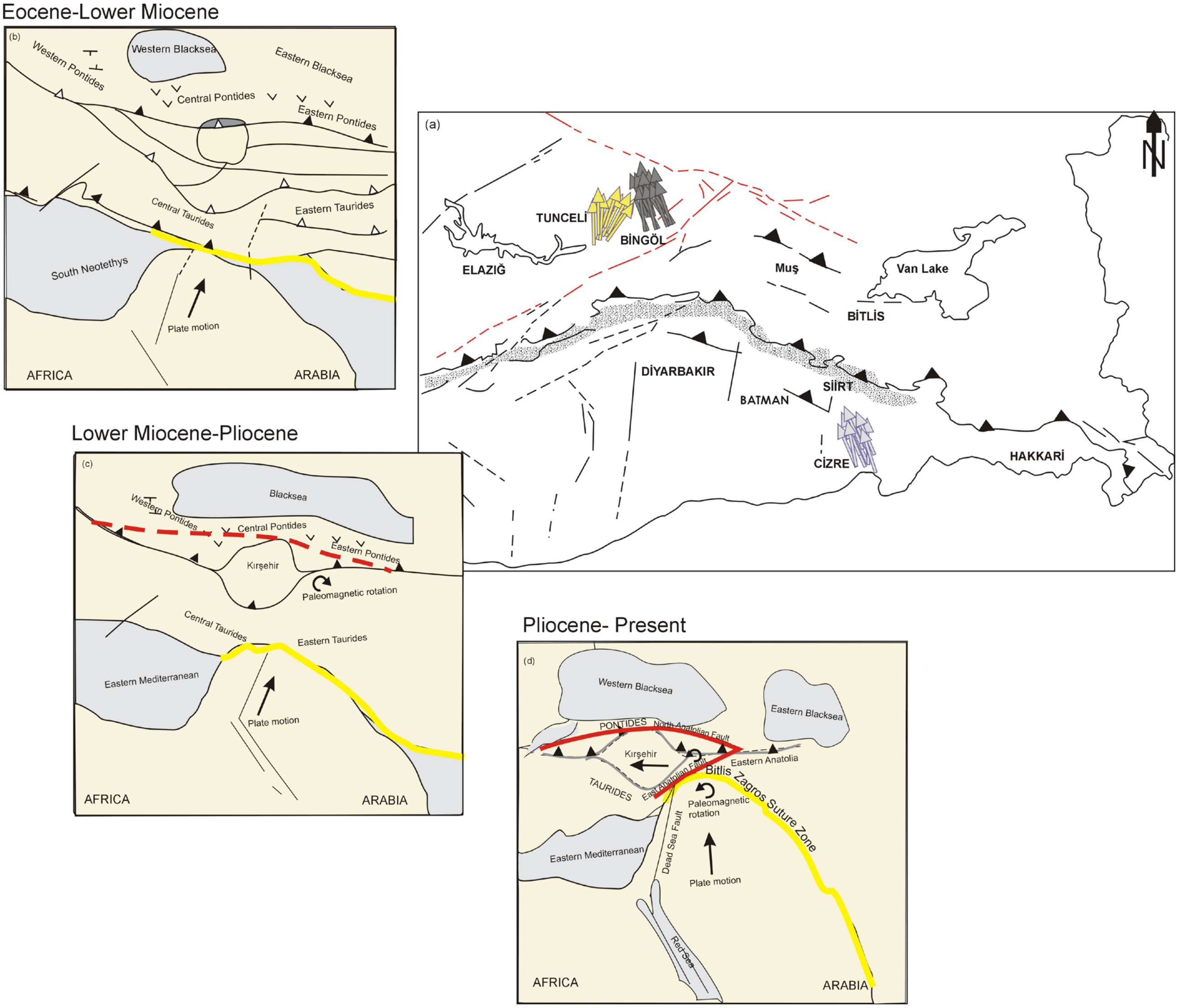


**Figure 6.** a) Paleomagnetic site mean directions (yellow arrow: Lower-Middle Miocene, dark gray: Pliocene, light gray: Quaternary). Tectonic evolution of in the Anatolian and Arabian Plate blocks during b) Eocene-Lower Miocene, c) Lower Miocene-Pliocene, d) Pliocene-Present (yellow line denotes the BZSZ, red lines denote the North (dashed line) and East Anatolian faults).

African Plate along the Aegean-Cyprus arc (Vidal et al., 2000; Schildgen et al., 2014; Özbakır and Govers Wortel, 2017; McPhee PJ and van Hinsbergen, DJJ 2019; Van Hinsbergen et al., 2020).

## 6. Conclusions

In this study, we have determined a clockwise rotation of 31.5° during the Early Miocene-Pliocene interval interpreted in terms of a NE-directed coherent movement of Anatolia together with Africa-Arabia. The timing and the oblique collision of the Arabian Plate with Anatolia along the BZSS resulted in clockwise rotations towards the Anatolian Plate and further northeast along the Caspian Sea, while the deformation of the African Plate contributed to the counterclockwise rotations within an area embraced by the Dead Sea, the Red Sea and to the region up to the collision front. The Pliocene and Quaternary counterclockwise rotations of 19.2° and 14.8°, in both Anatolia and Arabia, respectively accord with the indentation of the Arabian Plate towards the northwest accompanying the westward tectonic escape of Anatolia. Tectonic slip on the North and East Anatolian faults has subsequently dominated motions influencing the region during Pliocene and Quaternary times.

**Acknowledgement**
The authors appreciate Burak Semih ÇABUK for assisting in the laboratory measurements. We would like to thank Levent MESCI and Fikret KOCBULUT for supporting equipment in the field. This study was supported by the Scientific Research Projects Coordination Unit of İstanbul University–Cerrahpaşa with project number FBA-2019-33741. We are grateful to Dr. John Piper and the anonymous reviewer for their valuable scientific suggestions that improved the manuscript.

## References

Abou Deeb JM, Tarling DH (2005). A palaeomagnetic study of the volcanic rocks of El945 Mane mountain, south of Damascus, Syria. Geofisica Internacional, 44: 187-195. ISSN: 0016-7169.

Agostini S, Yilmaz Savaşçin M, Di Giuseppe P, Di Stefano F, Karaoğlu Ö et al. (2019). Neogene volcanism in Elazığ-Tunceli area (eastern Anatolia): geochronological and petrological constraints. Italian Journal of Geosciences, 138 (3): 435-455. http://doi.org/10.3301/IJG.2019.18

Allen MB, Armstrong HA (2008). Arabia–Eurasia collision and the forcing of mid-Cenozoic global cooling. Palaeogeography, Palaeoclimatology, Palaeoecology, 265 (1-2): 52-58. https://doi.org/10.1016/j.palaeo.2008.04.021

Barka A, Kadinsky Cade K (1988). Strike slip fault geometry in Turkey and its influence on earthquake activity. Tectonics, 7: 663-684. https://doi.org/10.1029/TC007i003p00663

Beck MEJr (1980). Paleomagnetic record of plate-margin tectonic processes along the western edge of North America: Journal of Geophysical Research, 85: 7115-7131. http://doi.org/10.1029/JB085iB12p07115

Bozkurt E, Koçyiğit A (1996). The Kazova Basin: an active flower structure on the Almus Fault Zone, a splay fault system of the North Anatolian Fault Zone, Turkey. Tectonophysics, 265: 239–254. http://doi.org/10.1016/S0040-1951(96)00045-5

Bozkurt E (2001). Neotectonics of Turkey—a synthesis. Geodinamica Acta, 14: 3–30.

Berberian M, King GGP (1981). Towards a paleogeography and tectonic evolution of Iran: Canadian Journal of Earth Sciences, 18: 210–265. http://doi.org/10.1080/09853111.2001.11432432

Cavazza W, Albino I, Zattin M, Galoyan G, Imamverdiyev N et al. (2015). Thermochronometric evidence for Miocene tectonic reactivation of the Sevan–Akera suture zone (Lesser Caucasus): A far-field tectonic effect of the Arabia–Eurasia collision? Geological Society of London, Special Publication, 428 (1): 187–198. https://doi.org/10.1144/SP428.4

Cavazza W, Cattò S, Zattin M, Okay AI, Reiners P (2018). Thermochronology of the Miocene Arabia-Eurasia collisionzone of southeastern Turkey. Geosphere, 14: 2277-2293. https://doi.org/10.1130/GES01637.1

Cox A (1969). Geomagnetic Reversals: Although decreasing rapidly, the earth's magnetic field is probably not now reversing. Science, 163 (3864): 237-245. http://doi.org/10.1126/science.163.3864.237

Darin MH, Umhoefer JP (2022). Diachronous initiation of Arabia–Eurasia collision from eastern Anatolia to the southeastern Zagros Mountains since middle Eocene time. International Geology Review, 64 (18): 2653–2681. https://doi.org/10.1080/00206814.2022.2048272

Deenen MH, Langereis CG, van Hinsbergen DJ, Biggin AJ (2011). Geomagnetic secular variation and the statistics of palaeomagnetic directions. Geophysical Journal International, 186 (2): 509-520. http://doi.org/10.1111/j.1365-246X.2011.05050.x

Demarest HH (1983). Error analysis for the determination of tectonic rotation from paleomagnetic data. Journal of Geophysical Research, 88: 4321-4328. http://doi.org/10.1029/JB088iB05p04321

Dembo N, Hamiel Y, Gronot R (2021). Mechanical contrast and asymmetric distribution of crustal deformation across plate boundaries: Insights from the northern Dead Sea fault system. Geology, 49 (5): 498–503. https://doi.org/10.1130/G48342.1

Dewey JF, Hempton MR, Kidd WSF, Şaroğlu F, Şengör AMC (1986). Shortening of continental lithosphere: the neotectonics of Eastern Anatolia: a young collision zone. In: Coward MP, Ries AC (eds) Collision tectonics, vol 19. Geological Society of London Special Publication, pp 3–36. http://doi.org/10.1144/GSL.SP.1986.019.01.01

Emre Oİ, Duman TY (2007). The East Anatolian Fault: Structural pattern and relationship with the Dead Sea Transform, Eos Trans. AGU,88 (52), Fall Meeting Abstract T42B-01.

Ergintav S, Floyd M, Paradissis D, Karabulut H, Vernant P et al. (2023). New geodetic constraints on the role of faults and blocks vs. distribute strain in the Nubia-Arabia-Eurasia zone of active plate interactions. Turkish Journal of Earth Sciences, 32 (3): 248-261. http://doi.org/10.55730/1300-0985.1842

Faccenna C, Bellier O, Martinod J, Piromallo C, Regard V (2006). Slab detachment beneath eastern Anatolia: a possible cause for the formation of the North Anatolian Fault, Earth and Planetary Science Letters, 242: 85-97. http://doi.org/10.1016/j.epsl.2005.11.046

Fisher R (1953). Dispersion on a sphere. Proceedings of the Royal Society of London, Series A. Mathematical and Pysical Sciences 217 (1130): 295–305. https://doi.org/10.1098/rspa.1953.0064

Gülyüz E, Durak H, Özkaptan M, Krijgsman W (2020). Paleomagnetic constraints on the early Miocene closure of the southern Neo-Tethys (Van region; East Anatolia): Inferences

Gürsoy H, Tatar O, Piper JDA, Heimann A, Kocbulut F et al. (2009). Palaeomagnetic study of Tertiary volcanic domains in Southern Turkey and Neogene anticlockwise rotation of the Arabian Plate, Tectonophysics 465 (1-4): 114-127. https://doi.org/10.1016/j.tecto.2008.11.001

Gürsoy H, Piper JDA, Tatar O, Temiz H (1997). A palaeomagnetic study of the Sivas Basin, Central Turkey: crustal deformation during lateral escape of the Anatolian Block. Tectonophysics 271: 89–106. http://doi.org/10.1016/S0040-1951(96)00242-9

Gürsoy H, Tatar O, Piper JDA, Koçbulut F, Akpınar Z et al. (2011). Palaeomagnetic study of the Kepezdağ and Yamadağ volcanic complexes, central Turkey: Neogene tectonic escape and block definition in the central-east Anatolides. Journal of Geodynamics, 51 (5): 308-326. http://doi.org/10.1016/j.jog.20http://doi.org/10.07.004

Hall R (1976). Ophiolite emplacement and the evolution of the Taurus suture zone, southeastern Turkey. Geological Society America Bulletin 87: 1078–88. http://doi.org/10.1130/0016-7606(1976)87<1078:OEATEO>2.0.CO;2

Hempton MR (1987). Constraints on Arabian plate motion and extensional history of the Red Sea. Tectonics, 6 (6): 687-705. http://doi.org/10.1029/TC006i006p00687

Henry B, Homberg C, Mroueh M, Hamdan W, Higazi F (2010) Rotations in Lebanon inferred from new palaeomagnetic data and implications for the evolution of the Dead Sea Transform system, in Homberg, C., and Bachmann, M., eds., Evolution of the Levant Margin and Western Arabia Platform since the Mesozoic: Geological Society of London Special Publication 341: 269–285, https://doi.org/10.1144/ SP341.13

Herece Eİ, Acar Ş (2016). The geology of Upper Cretaceous-Tertiary sequences in the vicinity of Pertek (Tunceli). Maden Tetkik ve Arama Dergisi, 153: 1-43. https://doi.org/10.19111/bmre.38353

Hisarli ZM, Çinku MC, Ustaömer T, Keskin M, Orbay N (2016). Neotectonic deformation in the Eurasia–Arabia collision zone, the East Anatolian Plateau, E Turkey: evidence from palaeomagnetic study of Neogene–Quaternary volcanic rocks. International Journal of Earth Sciences, 105: 139-165. http://doi.org/10.1007/s00531-015-1245-4

Hubert Ferrari A, King G, Woerd JVD, Villa I, Altunel E et al. (2009). Long-term evolution of the North Anatolian Fault: new constraints from its eastern termination. Geological Society, London, Special Publications, 311 (1): 133-154. http://doi.org/10.1144/SP311.5

Hüsing SK, Zachariasse WJ, van Hinsbergen DJ, Krijgsman W, Inceöz M et al. (2009). Oligocene–Miocene basin evolution in SE Anatolia, Turkey: constraints on the closure of the eastern Tethys gateway. Geological Society, London, Special Publications, 311 (1): 107-132. http://doi.org/10.1144/SP311.4

Ibrahim EH, Odah HH, El Agami NL, El Enen MA (2000). Paleomagnetic and geological investigation into southern Sinai volcanic rocks and the rifting of the Gulf of Suez. Tectonophysics, 321 (3): 343-358. https://doi.org/10.1016/S0040-1951(00)00066-4

Innocenti F, Mazzuoli R, Pasquare G, Di Brozolo FR, Villari L (1976). Evolution of the volcanism in the area of interaction between the Arabian, Anatolian and Iranian plates (Lake Van, Eastern Turkey). Journal of Volcanology and Geothermal Research, 1 (2): 103-112. https://doi.org/10.1016/0377-0273(76)90001-9

Jolivet L, Faccenna C (2000). Mediterranean extension and the Africa-Eurasia collision, Tectonics, 19 (6): 1095-1106. https://doi.org/10.1029/2000TC900018

Jolivet L, Faccenna C, Piromallo C (2009). From mantle to crust: Stretching the Mediterranean, Earth Planetary Science Letteters, 285: 198– 209 https://doi.org/10.1016/j.epsl.2009.06.017

Karaoğlan F, Parlak O, Hejl E, Neubauer F, Kloetzli U (2016). The temporal evolution of the active margin along the Southeast Anatolian Orogenic Belt (SE Turkey): Evidence from U–Pb, Ar–Ar and fission track chronology. Gondwana Research, 33: 190-208. http://doi.org/10.1016/j.gr.2015.12.011

Karaoğlu Ö, Gülmez F, Göçmengil G, Lustrino M, Di Giuseppe P et al. (2020). Petrological evolution of Karlıova-Varto volcanism (Eastern Turkey): Magma genesis in a transtensional triple-junction tectonic setting. Lithos, 364: 105524. http://doi.org/10.1016/j.lithos.2020.105524

Karig DE, Kozlu H (1990). Late Palaeogene Evolution of the Triple Junction Region Near Maras¸ south-central Turkey. Journal of the Geological Society, London 147: 1023–1034. https://doi.org/10.1144/gsjgs.147.6.1023

Kaya A (2016). Tectono-stratigraphic reconstruction of the Keban metamorphites based on new fossil findings, Eastern Turkey. Journal of African Earth Sciences, 124: 245-257. https://doi.org/10.1016/j.jafrearsci.2016.09.032

Kayın S, İşseven T (2023). New paleomagnetic results from Neogene to Quaternary volcanic rocks of north of the Lake Van, Eastern Turkey. Scientific Reports 13: 12206. https://doi.org/10.1038/s41598-023-39492-w

Kellogg KS, Reynolds RL (1983). Opening of the Red Sea: constraints from a palaeomagnetic study of the As Sarat volcanic field, south-western Saudi Arabia. Geophysial Journal International, 74 (3): 649-665. https://doi.org/10.1111/j.1365-246X.1983.tb01898.x

Keskin M, Pearce JA, Mitchell JG (1998). Volcano-stratigraphy and geochemistry of collision-related volcanism on the Erzurum–Kars Plateau, North Eastern Turkey. Journal of Volcanology and Geothermal Research, 85 (1–4): 355–404. https://doi.org/10.1016/S0377-0273(98)00063-8

Keskin M (2003). Magma generation by slab steepening and breakoff beneath a subduction-accretion complex: An alternative model for collision-related volcanism in Eastern Anatolia, Turkey, Geophysical Research Letters, 30 (24): 8046 https://doi.org/10.1029/2003GL018019

Kirschvink JL (1980). The least squares line and plane and the analysis of paleomagnetic data, Geophysical Journal of the Royal Astronomical Society 62: 699-718. https://doi.org/10.1111/j.1365-246X.1980.tb02601.x

Kissel C, Laj C, Poisson A, Görür N (2003). Paleomagnetic reconstruction of the Cenozoic evolution of the eastern Mediterranean, Tectonophysics, 362: 199–217, https://doi.org/10.1016/S0040-1951(02)00638-8

Koçbulut F, Akpınar Z, Tatar O, Piper JDA, Roberts AP (2013). Palaeomagnetic study of the Karacadağ Volcanic Complex, SE Turkey: monitoring Neogene anticlockwise rotation of the Arabian Plate, Tectonophysics 608: 1007-1024. http://doi.org/10.1016/j.tecto.2013.07.013

Lebedev VA, Sharkov EV, Keskin M, Oyan V (2010). Geochronology of Late Cenozoic volcanism in the area of Van Lake, Turkey: an example of development dynamics for magmatic processes. Doklady Earth Sciences, 433 (2): 1031–1037. http://doi.org/10.1134/S1028334X1008009X

Lebedev VA, Chugaev AV, Ünal E, Sharkov EV, Keskin M (2016) Late pleistocene tendürek volcano (eastern Anatolia, Turkey). II. Geochemistry and petrogenesis of the rocks. Petrology, 24: 234-270. https://doi.org/10.1134/S0869591116030048

Lowrie W (1990). Identification of ferromagnetic minerals in a rock by coercivity and unblocking temperature properties. Geophysical Research Letters, 17: 159–162. https://doi.org/10.1029/GL017i002p00159

Mahatsente R, Önal G, Çemen I (2018). Lithospheric structure and the isostatic state of Eastern Anatolia: Insight from gravity data modelling. Lithosphere, 10 (2): 279-290. https://doi.org/10.1130/L685.1

Mantovani E, Viti M, Babbucci D, Tamburelli C, Albarello D (2006). Geodynamic connection between the indentation of Arabia and the Neogene tectonics of the Central–Eastern Mediterranean region. In: Dilek, Y. and Pavlides, S., Eds., Post-Collisional Tectonics and Magmatism in the Mediterranean Region and Asia, Geological Society of America Special Papers 409, Boulder, 15-41. https://doi.org/10.1130/2006.2409(02)

Matthews KJ, Maloney KT, Zahirovic S, Williams SE, Seton M et al. (2016). Global plate boundary evolution and kinematics since the late Paleozoic: Global and Planetary Change, 146: 226–250 https://doi.org/10.1016/j.gloplacha.2016.10.002

McClusky S, Balassanian S, Barka A, Demir C, Ergintav S et al. (2000). Global Positioning System constraints on plate kinematics and dynamics in the eastern Mediterranean and Caucasus, Journal of Geophysical Research, 105: 5695-720. http://doi.org/10.1029/1996JB900351

McElhinny MW, McFadden PL (1997). Palaeosecular variation over the past 5 Myr based on a new generalized database. Geophysical Journal International, 131 (2): 240-252. https://doi.org/10.1111/j.1365-246X.1997.tb01219.x

McKenzie D (1978). Some remarks on the development of sedimentary basins. Earth and Planetary Science Letters, 40 (1): 25-32. https://doi.org/10.1016/0012-821X(78)90071-7

McPhee PJ, van Hinsbergen DJJ (2019). Tectonic reconstruction of Cyprus reveals Late Miocene continental collision of Africa and Anatolia, Gondwana Research, 68: 158-173. https://doi.org/10.1016/j.gr.2018.10.015

McQuarrie N, Stock JM, Verdel C, Wernicke BP (2003). Cenozoic evolution of Neotethys and implications for the causes of plate motions: Geophysical Research Letters, 30 (20): 2036. https://doi.org/10.1029/2003GL017992

McQuarrie N, van Hinsbergen DJJ (2013). Retrodeforming the Arabia-Eurasia collision zone: Age of collision versus magnitude of continental subduction: Geology, 41: 315-318. https://doi.org/10.1130/G33591.1

Medved I, Polat G, Koulakov I (2021). Crustal structure of the Eastern Anatolia Region (Turkey) based on seismic tomography. Geosciences, 11 (2): 91. https://doi.org/10.3390/geosciences11020091

MTA (2002). 1:500.000 Ölçekli Türkiye Jeoloji Haritaları (Erzurum Paftası), General Directorate of Mineral Research and Exploration, Ankara.

MTA (2007). Cizre İlçesinin 1/100.000'lik Jeoloji Haritası, Maden Tetkik ve Arama Genel Müdürlüğü, Jeoloji Etüdleri Dairesi, Ankara

Okay AI (1984). Distribution and characteristics of the north-west Turkish blueschists. Geological Society, London, Special Publications, 17 (1): 455-466. https://doi.org/10.1144/GSL.SP.1984.017.01.33

Okay AI, Zattin M, Cavazza W (2010). Apatite fission-track data for the Miocene Arabia-Eurasia collision: Geology, 38: 35–38. http://doi.org/10.1130/G30234.1

Özbakır AD, Govers Wortel RR (2017). Active faults in the Anatolian-Aegean plate boundary region with Nubia. Turkish Journal of Earth Sciences, 26: 30-56. https://doi.org/10.3906/yer-1603-4

Özdemir Y, Güleç N (2014). Geological and geochemical evolution of the Quaternary Süphan stratovolcano, Eastern Anatolia, Turkey: evidence for the lithosphere–asthenosphere interaction in post-collision volcanism. Journal of Petrology 55: 37–52. https://doi.org/10.1093/petrology/egt060

Parlak O, Rızaoğlu T, Bağcı U, Karaoğlan F, Höck V (2009). Tectonic significance of the geochemistry and petrology of ophiolites in the southeast Anatolia, Turkey. Tectonophysics, 473: 173-187. https://doi.org/10.1016/j.tecto.2008.08.002

Parlak O, Karaoğlan F, Rizaoğlu T, Nurlu N, Bağci U et al. (2013). Petrology of the İspendere (Malatya) ophiolite from the Southeast Anatolia: implications for the Late Mesozoic evolution of the southern Neotethyan ocean. Geological Society, London, Special Publications, 372 (1): 219-247. https://doi.org/10.1144/SP372.11

Pearce JA, Bender JF, DeLong SE, Kidd WSF, Low PJ et al. (1990). Genesis of collision volcanism in Eastern Anatolia, Turkey, In: P. LeFort, J.A. Pearce and A. Pecher (eds); Collision Magmatism, Journal of Volcanology and Geothermal Research, 44: 184 – 229. http://doi.org/10.1016/0377-0273(90)90018-B

Perinçek D (1979). The geology of Hazro-Koruday-Çüngüş- Maden-Ergani-Hazır-Elazığ-Malatya area. Guide book, Türkiye Jeoloji Kurumu yayını, Ankara, 34s.

Philip H, Cisternas A, Gvishiani A, Gorshkov A (1989). The Caucasus: an actual example of the initial stages of continental collision. Tectonophysics, 161 (1-2): 1-21. http://doi.org/10.1016/0040-1951(89)90297-7

Reilinger RE, McClusky SC, Souter BJ (1997a). Preliminary estimates of plate convergence in the Caucasus collision zone from GPS measurements, Geophysical Research Letters, 24: 1815–1818. http://doi.org/10.1029/97GL01672

Reilinger RE, McClusky SC, Oral MB, King RW, Toksoz MN et al. (1997b). Global Positioning System measurements of present-day crustal movements in the Arabia-Africa-Eurasia plate collision zone. Journal of Geophysical Research: Solid Earth, 102 (B5): 9983-9999. https://doi.org/10.1029/96JB03736

Reilinger RE, McClusky SC, Vernant P, Lawrances S, Ergintav S et al. (2006). GPS Constraints on Continental Deformation in the Africa Arabia-Eurasia Continental Collision Zone and Implications for the Dynamics of Plate Interactions, Journal of Geophysical Research 111: B05411, https://doi.org/10.1029/2005JB004051

Robertson AHF, Parlak O, Rızaoğlu T, Ünlügenç U, İnan N et al. (2007). Tectonic evolution of the South Tethyan ocean: Evidence from the Eastern Taurus Mountains (Elazığ region, SE Turkey), In: Ries, A.C., Butler, R.W.H. & Graham, R.H. (eds) Deformation of the Continental Crust: The Legacy of Mike Coward, Geological Society, London, Special Publications, 272: 231–270. http://doi.org/10.1144/GSL.SP.2007.272.01.14

Rolland Y, Perincek D, Kaymakci N, Sosson M, Barrier E et al. (2012). Evidence for ~80–75 Ma subduction jump during Anatolide–Tauride–Armenian block accretion and ~ 48 Ma Arabia–Eurasia collision in Lesser Caucasus–east Anatolia. Journal of Geodynamics, 56-57: 76–85. https://doi.org/10.1016/j.jog.2011.08.006

Roperch P, Bonhommet N (1986). Paleomagnetism of Miocene volcanism from South Syria. Journal of Geophysicics, 59: 98-102. https://hall.science/hal-03522466

Sandvol E, Turkelli N, Barazangi M (2003). The Eastern Turkey Seismic Experiment: the study of a young continent–continent collision Geophysical Research Letters, 30 (24) (2003): 8038. https://doi.org/10.1029/2003GL018912

Schildgen TF, Yıldırım C, Cosentino D, Strecker MR (2014). Linking slab break-off, Hellenic trench retreat, and uplift of the Central and Eastern Anatolian plateaus. Earth Science Reviews, 128: 147-168. https://doi.org/10.1016/j.earscirev.2013.11.006

Su H, Zhou J (2020). Timing of Arabia-Eurasia collision: Constraints from restoration of crustal-scale cross-sections. Journal of Structural Geology, 135: 104041. http://doi.org/10.1016/j.jsg.2020.104041

Şaroğlu F, Yılmaz Y (1991). Geology of the Karlıova region: intersection of the North Anatolian and East Anatolian transform faults. Bulletin Technical University Istanbul, 44: 475-493.

Şengör AMC, Kidd WSF (1979). The post-collisional tectonics of the Turkish-Iranian Plateau and a comparison with Tibet, Tectonophysics, 55: 361-376. https://doi.org/10.1016/0040-1951(79)90184-7

Şengör AMC, Yılmaz Y (1981). Tethyan evolution of Turkey: a plate tectonic approach, Tectonophysics 75: 181–241. http://doi.org/10.1016/0040-1951(81)90275-4

Şengör AMC, Görür N, Şaroğlu F (1985). Strike-slip faulting and related basin formation in zones of tectonic escape: Turkey as a case study. In: Biddle KT, Christie-Blick N (eds) Strike-slip deformation, basin formation and sedimentation society of economic paleontologists and mineralogists special publication 37: 227–264.

Şengör AMC, Ozeren S, Zor E, Genç T (2003). East Anatolian high plateau as a mantle-supported, N-S shortened domal structure, Geophysical Research Letters 30 (24): https://doi.org/10.1029/2003GL017858

Şengör AMC, Tüysüz O, İmren C, Sakınç M, Eyidoğan H et al. (2005). The North Anatolian Fault: A New Look: Annual Review of Earth Panetary Science, 33: 37-112. https://doi.org/10.1146/annurev. earth.32.101802.120415

Şengül Uluocak E, Göğüş OH, Pysklywec RN, Chen B (2021). Geodynamics of East Anatolia-Caucasus Domain: Inferences From 3D Thermo-Mechanical Models, Residual Topography, and Admittance Function Analyses. Tectonics, 40 (12) e2021TC007031._ https://doi.org/10.1029/2021TC007031

Skobeltsyn G, Mellors R, Gök R, Türkelli N, Yetirmishli G et al. (2014). Upper mantle S wave velocity structure of the East Anatolian-Caucasus region. Tectonics, 33 (3): 207-221. https://doi.org/10.1002/2013TC003334

Tatar O, Piper JDA, Gürsoy H, Heimann A, Koçbulut F (2004). Neotectonic deformation in the transition zone between the Dead Sea Transform and the East Anatolian Fault Zone, Southern Turkey: a palaeomagnetic study of the Karasu Rift Volcanism. Tectonophysics, 385 (1-4): 17-43. https://doi.org/10.1016/j.tecto.2004.04.005

Tauxe L (2005). Paleomagnetic Principles and Practice, 299 Springer, New York. ISBN: 0306481286, 9780306481284

Tolun N (1960). Stratigraphy and tectonics of Southeastern Anatolia. Révue de la Faculté des Sciences de l'Université D'İstanbul, Tome XXV, 3-4 (B): 204-264. https://doi.org/10.19111/bulletinofmre.401216

Torsvik TH, Van der Voo R, Preeden U, Mac Niocaill C, Steinberger B et al. (2012). Phanerozoic polar wander, paleogeography and dynamics. Earth Science Reviews, 114 (3-4): 325–368. https://doi.org/10.1016/j.earscirev.2012.06.007

Türkoğlu E, Unsworth M, Çağlar İ, Tuncer V, Avşar Ü (2008). Lithospheric structure of the Arabia-Eurasia collision zone in eastern Anatolia: Magnetotelluric evidence for widespread weakening by fluids?. Geology, 36 (8): 619-622. http://doi.org/10.1130/G24683A.1

Van der Boon A, Kuiper KF, Villa G, Renema W, Meijers MJM et al. (2017). Onset of Maikop sedimentation and cessation of Eocene arc volcanism in the Talysh Mountains, Azerbaijan. Geological Society London, Special Publications 428: 145–169. http://doi.org/10.1144/SP428.3

Van Hinsbergen DJ, Torsvik TH, Schmid SM, Maţenco LC, Maffione M et al. (2020). Orogenic architecture of the Mediterranean region and kinematic reconstruction of its tectonic evolution since the Triassic. Gondwana Research, 81: 79-229. https://doi.org/10.1016/j.gr.2019.07.009

Vidal N, Klaeschen D, Kopf A, Docherty C, Von Huene R et al. (2000). Seismic images at the convergence zone from south of Cyprus to the Syrian coast, eastern Mediterranean. Tectonophysics, 329 (1-4): 157-170. https://doi.org/10.1016/S0040-1951(00)00194-3

Vincent SJ, Morton AC, Carter A, Gibbs S, Barabadze TG (2007). Oligocene uplift of the Western Greater Caucasus: an effect of initial Arabia–Eurasia collision. Terra Nova, 19 (2): 160-166. https://doi.org/10.1111/j.1365-3121.2007.00731.x

Westaway RWC, Arger J (1996). The Gölbaşı Basin, Southeastern Turkey: A Complex Discontinuity in a Major Strike-Slip Fault Zone. Journal of the Geological Society 153: 729-744. https://doi.org/10.1144/gsjgs.153.5.0729

Whitney DI, Delph JR, Thomson SN, Beck SL, Brocard GY et al. (2023). Breaking plates: Creation of the East Anatolian fault, the Anatolian plate, and a tectonic escape system. Geology 2023 https://doi.org/10.1130/G51211.1

Yılmaz Y (1990a). Comparison of young volcanic associations of western and eastern Anatolia formed under a compressional regime: a review. Journal of Volcanology and Geothermal Research, 44 (1-2): 69-87. https://doi.org/10.1016/0377-0273(90)90012-5

Yılmaz Y (1990b). Allochthonous terranes in the Tethyan Middle East: Anatolia and the surrounding regions. Philosophical Transactions of the Royal Society of London. Series A, Mathematical and Physical Sciences, 331 (1620): 611-624. https://doi.org/10.1098/rsta.1990.0093

Yılmaz Y (1993). New evidence and model on the evolution of the Southeast Anatolian orogen, Geological Society of America Bulletin, 105: 251-71. https://doi.org/10.1130/0016-7606(1993)105<0251:NEAMOT>2.3.CO;2

Yılmaz Y, Güner Y, Şaroğlu F (1998). Geology of the Quaternary volcanic centers of the east Anatolia, Journal of Volcanology and Geothermal Research 85: 173-210. https://doi.org/10.1016/S0377-0273(98)00055-9

Yılmaz Y (2019). Southeast Anatolian Orogenic Belt revisited (geology and evolution). Canadian Journal of Earth Sciences, 56 (11): 1163-1180. https://doi.org/10.1139/cjes-2018-0170

Zijderveld JDA (1967). AC demagnetization of rocks: analysis of results, In: D.W. Collison, K.M. Creer and S.K. Runcorn (Editors), Methods in Paleomagnetism. Elsevier, Amsterdam, 245-286. https://doi.org/10.1016/B978-1-4832-2894-5.50049-5

Zijderveld JDA (1968). Natural remanent magnetizations of some intrusive rocks from the Sør Rondane Mountains, Queen Maud Land, Antarctica. Journal of Geophysical Research, 73 (12): 3773-3785. https://doi.org/10.1029/JB073i012p03773

Zor E, Sandvol E, Gürbüz C, Türkelli N, Seber D et al. (2003). The crustal structure of the East Anatolian plateau (Turkey) from receiver functions. Geophysical Research Letters, 30 (24). https://doi.org/10.1029/2003GL018192